Eighth Australasian Fluid Mechanics Conference, University of Newcastle, N.S.W., 28 November/2 December 1983.

BUOYANT PLUME RISE: COMPARISON BETWEEN PROTOTYPE & A WIND TUNNEL MODEL

A.J. CHAMBERS
DEPT. OF MECH. ENG.
UNI. OF NEWCASTLE
NSW. 2308 AUSTRALIA

A.J. BOWEN
DEPT. OF MECH. ENG.
UNI. OF CANTERBURY
CHRISTCHURCH, NEW ZEALAND

H.A. BRIDGMAN
DEPT. OF GEOGRAPHY
UNI. OF NEWCASTLE
NSW. 2308 AUSTRALIA

SUMMARY A comparison is made between the buoyant plume rise and vertical spread from a coal fired power station stack and a 1/440 scale model of the stack. The agreement between plume rise is qualitatively in agreement using physical scaling but appears to improve when scaled for the buoyant region using an appropriate length scale. Buoyant plume rise and vertical spread from the power station and model satisfies the 2/3 power law. The calculated plume breakup distance from the power station is less than 4 km and is similar to the distance where visual tracking ceased.

NOMENCLATURE

D	internal exit diameter of stack
g	gravity constant
ΔH	height of plume/jet centreline above stack exit
H_s	stack height
H	$= H_s + \Delta H$; effective stack height
ℓ_b	buoyancy length
ℓ_m	momentum length
L	length scale
Q	$= g\, \overline{w'T'}/T = w_*^3/z_i$; surface kinematic heat flux
T	mean temperature
ΔT	$= T_s - T_a$; exit temperature from stack relative to ambient
u_*	friction velocity
U	mean longitudinal velocity
w	vertical spread of plume/jet
w_*	convective layer scaling velocity
W	mean vertical velocity
x	downwind direction from stack
z_i	planetary boundary layer thickness
ρ	density of gas
λ_L	model geometric scale
λ_u	model vertical scale
ν	kinematic viscosity

Subscripts:

a	ambient
B	breakup of plume
M	model
p	prototype
s	exit of stack

INTRODUCTION

To gain confidence in the use of physical models it is useful to compare model and prototype results for a simple terrain. Here the plume characteristics of a 1/440 physical model of a Liddell power station stack are compared to the power station plume. Use of similarity arguments for the "bent over" buoyant plume region are examined.

1. THEORY

1.1 Physical Modelling of Plume Behaviour

To obtain exact modelling of the plume with a geometric scale of $\lambda_L = L_M/L_p$, the following physical parameters should be satisfied:

$$\left.\begin{aligned} D_M/D_p &= \lambda_L \\ (Dg/U^2)_M &= (Dg/U^2)_p \\ (\rho_s/\rho_a)_M = (\rho_s/\rho_a)_p \qquad & (W_s/U)_M = (W_s/U)_p \\ (DW_s/\nu_s)_M &= (DW_s/\nu_s)_p \end{aligned}\right\} \quad (1)$$

The velocity scale to satisfy Froude number similarity is

$$\lambda_u = \sqrt{\lambda_L} \quad . \qquad (2)$$

A geometric scale of $\lambda_L = 1:440$ gives a corresponding velocity scale of $\lambda_u = 1:21$. The full scale wind speeds of interest are in the range 4-20 m/s. For exact modelling wind speeds in the range 0.19-1.0 m/s are required. It is not possible to model the stack Reynolds number.

1.2 Bent Over Plume in an Ambient Cross Flow

Similarity arguments, for example Fisher et al (1979, Ch. 9) indicate for a buoyant bent over plume in a neutral cross-flow

$$\frac{\Delta H}{\ell_b} = C_1 \left(\frac{x}{\ell_b}\right)^{2/3} , \qquad (3)$$

and for a bent over jet

$$\frac{\Delta H}{\ell_m} = C_2 \left(\frac{x}{\ell_m}\right)^{1/3} . \qquad (4)$$

The buoyancy length is given by

$$\ell_b = \frac{\pi\, g\, \frac{\Delta T}{T_s}\, W_s\, \frac{D^2}{4}}{U^3} \qquad (5)$$

and the momentum length by

$$\ell_m = \frac{\left(\pi\, W_s^2\, \frac{D^2}{4}\right)^{1/2}}{U} \quad . \qquad (6)$$

For a bent over plume or jet in a cross flow a characteristic radius is expected to be proportional to the vertical rise as ΔH is the only similarity length scale, thus w is expected to be proportional to $(x/\ell_b)^{2/3}$ and $(x/\ell_m)^{1/3}$ respectively for a buoyant and momentum dominated bent over plume.

2. EXPERIMENTAL DESCRIPTION

2.1 The Prototype

The Liddell power station is located in the middle Hunter Valley in undulating country about 100 km northwest of Newcastle in eastern New South Wales. The power station is a 2000 MW coal burning facility with boiler emissions released from two 168 m high stacks (D = 8.67 m, $W_s \simeq 20$ m/s, $\Delta T \simeq 100°C$), separated by 150 m. Plume rise measurements were obtained during an inten-

sive study of the dispersion characteristics of the Liddell power station plume.

Measurements of the height of the plume centreline above the ground for different downwind distances were obtained using a theodolite fitted with an open sight and time lapse photography (16 mm wide angle lens cinefilm with a 15 s or 60 s delay between frames). Details are provided in Bridgman and Chambers (1981) and Chambers and Bridgman (1983). There was reasonable agreement of ΔH measured using theodolite and time lapse film.

The wind speed at the effective stack height was estimated from Mt. Arthur (11.3 km to west and 360 m above the stack base) and Liddell (about 10 m above stack base) wind data using a conventional power law relation between velocity and height. Estimates of U from the film agreed reasonably well with these results. W_s and ΔT were estimated from power station data provided by the New South Wales Electricity Commission.

2.2 The Model

The model was tested in the atmospheric boundary layer wind tunnel (cross section 1.22 × 1.22 m, length 12.2 m) in the Department of Mechanical Engineering at the University of Canterbury, New Zealand. A full description of the wind tunnel and operating characteristics is given by Raine (1974). In the test section the roof panels were adjusted so that the velocity remained constant in the streamwise direction. The free stream velocity (turbulence level 0.2%) was measured using a propeller anemometer (Flay, 1978) which was calibrated for low velocities at the Ministry of Works current meter testing facilities. The low speed relation between frequency and velocity follow that suggested by Jackson (1980).

The stack model was a 280 mm long, 40 mm diameter glass tube. A nozzle, D = 20 mm, was attached to the stack exit. Gas entered the stack from two supplies. The flow rate for both supplies was measured using a rotometer, pressure gauge and mercury in glass thermometer. The primary air flow was heated before entering the stack. The secondary supply was nitrogen which was passed to a smoke generator and oil trap before entering the stack at its base. The flow rate was calibrated using unheated gas and a hot wire located at the jet exit. The exit temperature was measured using a thermocouple and controlled by adjusting the power to the primary air heat exchanger. The jet exit was located 0.2 m above the test section floor and the exit Reynolds number was about 1600. A cap was located over the nozzle to provide a 60 mm diameter concentric flat surface surrounding the nozzle exit.

To track the plume boundaries, photographs with time exposures of 60 to 120 s were taken using a 35 mm wide angle lens camera. The area to be photographed was blacked out and the plume was made visible by side lighting. The lights were located (35 mm projector and flood lights) in the wind tunnel far downstream (~ 6 m).

3. RESULTS

Tables 1 and 2 summarise the conditions for the prototype and model study. Included in Table 1 is the parameter U/w_* which indicates convective conditions when $1.5 < U/w_* < 6$ (Deardorff and Willis, 1975). w_* was estimated from radiation measurements using a procedure suggested by Venkatram (1978). For the model, usually two sets of data were collected as a sensitivity test and these are displayed in the figures as open and closed symbols.

Figure 1 compares the physical modelling for the two flows. There is qualitative agreement between model and prototype, ΔH decreases as U/W_s increases. The downwind distance that the plume is measured is smaller for the model as the wind tunnel size restricts the spread and/or rise of the plume for x/D greater than 125.

TABLE 1 PROTOTYPE STUDY PARAMETERS

U m/s	U/W_s	ℓ_b m	ℓ_m m	Neutral x_B/ℓ_b (9)	Convective[§] x_B/ℓ_b (10)	U/w_*	Symbol
2.5	0.15	220	51	----[†]	8.1	1.3	○
2.5	0.18	180	43	----	5.7	1.0	+
3.2	0.19	100	31	----	26	1.9	·
3.6	0.25	62	30	----	20	1.4	□
3.7	0.26	57	27	----	24	1.5	×
5.4	0.29	24	23	----	110	2.6	▽
5.5	0.33	20	23	----	140	2.8	△
5.7	0.34	18	16	----	140	2.7	●
9.7	0.47	4.6	14	820	840	4.7	*
6.8	0.51	8.6	15	600	----	---	▲
11.1	0.54	3.0	14	1000	1100	4.7	■
7.3	0.73	2.2	10	1200	1100	4.3	▼

[†] Not applicable

[§] z_i = 1500 m (assumed)

TABLE 2 MODEL STUDY PARAMETERS

U m/s	U/W_s	ℓ_b (ΔT = 100°C) m × 10^{-3}	ℓ_m m × 10^{-3}	Symbol (ΔT = 100°C)	Symbol (ΔT = 15°C)
0.25	0.21	63	85	□	□
0.35	0.29	23	61	△	△
0.50	0.42	6.9	42	○	○
0.75	0.62	2.2	28	▽	○
1.00	0.83	0.91	21	○	▽

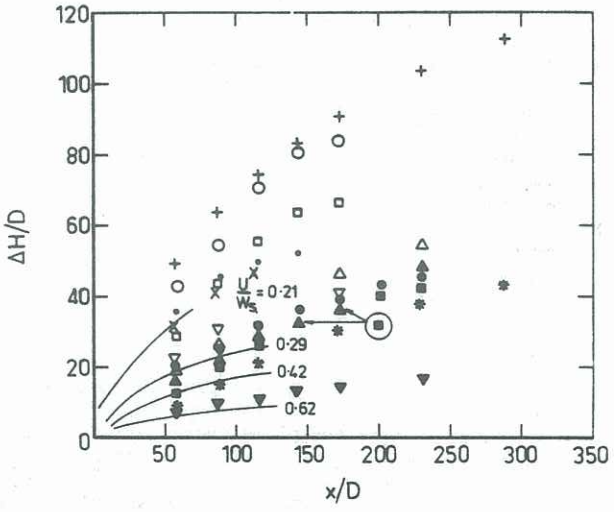

Figure 1 Physical modelling of buoyant plume : model and prototype. Solid lines - model at given U/W_s. See Table 1 for symbols.

When the prototype and model plumes rise, and vertical spread, Figures 2 to 5, are non-dimensionalised by an appropriate buoyancy length (5), the agreement between results improves. The buoyant plume rise is approximately equal for both model and prototype and satisfy the 2/3 power law and roughly fall within a band [$0.82 < C_1 < 1.3$, (3)] suggested by Briggs (1975). The vertical plume spreading for the prototype is in the range of one to two times the plume rise and w appears to increase with U/W_s. For the model $w \simeq \Delta H$ for U/W_s less than or equal to 0.4. The agreement between the plume spreading

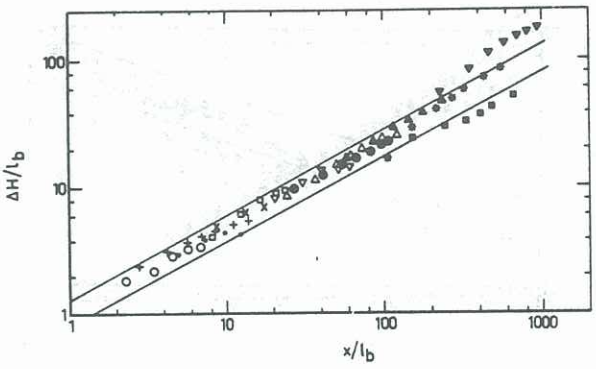

Figure 2 Centreline for buoyant plume : prototype. See Table 1 for symbols. Solid lines (3) with C_1 = 0.82 and 1.3.

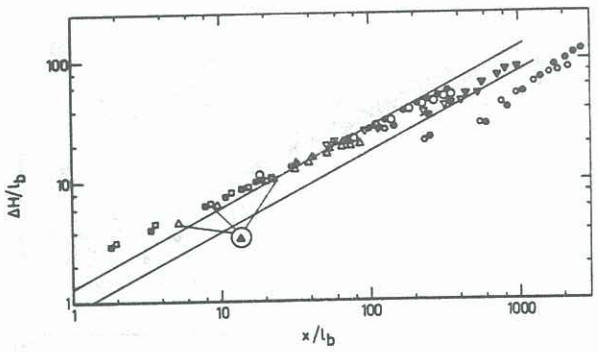

Figure 3 Centreline for buoyant plume : model. See Table 2 for symbols. Solid lines (3) with C_1 = 0.82 and 1.3.

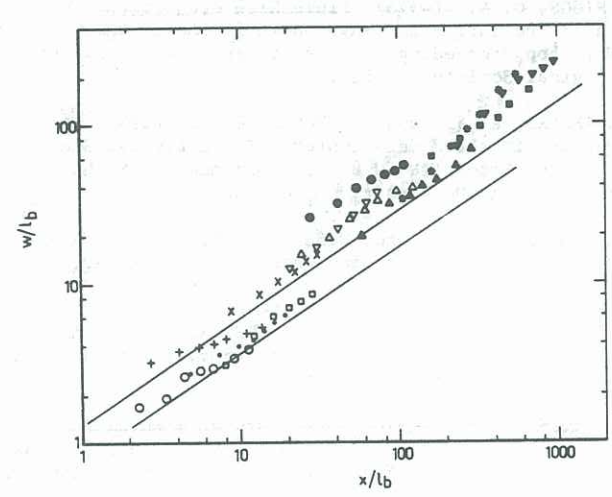

Figure 4 Vertical spread and buoyant plume : prototype. See Table 1 for symbols. Solid lines (3) with C_1 = 0.82 and 1.3.

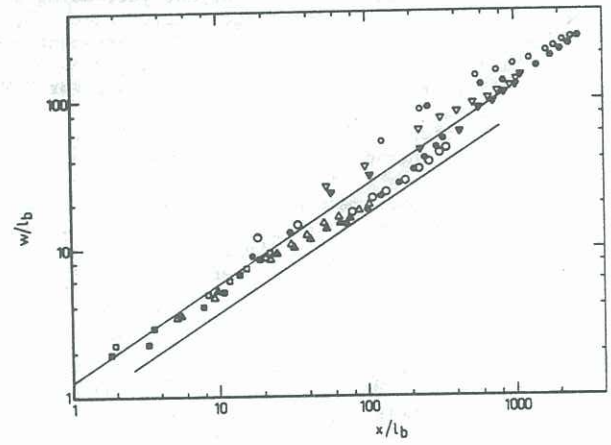

Figure 5 Vertical spread buoyant plume : model. See Table 2 for symbols. Solid lines (3) with C_1 = 0.82 and 1.3.

for model and prototype is at first surprising and suggests that buoyancy dominates the plume spreading and correct modelling of the atmospheric boundary layer is not important.

Briggs (1975) suggested that breakup of the plume occurred when the dissipation within the plume was equal to the surrounding atmospheric dissipation. This is expected to be the location where atmospheric turbulence begins to dominate the dispersion process. Equations given in Hanna et al (1982) for the final plume rise can be expressed in terms of ℓ_b for neutral conditions (with $u_*/U \simeq 16$) as

$$\frac{\Delta H_B}{\ell_b} = 29 \left(\frac{H_s}{\ell_b}\right)^{1/3} \qquad (7)$$

and for convective conditions (a tentative estimate)

$$\frac{\Delta H_B}{\ell_b} = 1.5 \left\{\frac{z_i}{\ell_b}\left(\frac{U}{w_*}\right)^3\right\}^{2/5} . \qquad (8)$$

Using (3) with C_1 = 1.1, the downwind position of breakup is, for neutral conditions

$$\frac{x_B}{\ell_b} = 135 \left(\frac{H_s}{\ell_b}\right)^{1/2} , \qquad (9)$$

and convective conditions

$$\frac{x_B}{\ell_b} = 1.6 \left\{\frac{z_i}{\ell_b}\left(\frac{U}{w_*}\right)^3\right\}^{2/5} . \qquad (10)$$

Estimates of x_B are listed in Table 1. Only values for high wind speeds are listed for the neutral case, for convective conditions z_i was assumed to be 1500 m, the mean of several z_i estimates obtained from aircraft vertical temperature profiles.

Generally the plume was visible for x from 1.5 to 2.5 km. Using (9) the mean value of x_B is 4 km. With (10) the mean value of x_B is 2.3 km and ranges from 1.0 to 3.9 km. There is some correlation between x_B given by (10) and where the tracking of the plume ceased. However the tracking of the plume from photographs ceased when the lower boundary came to ground or when it could not be distinguished from the background. Generally x_B is greater than the distance the plume was tracked downwind and thus atmospheric turbulence is expected to have little effect on the plume boundaries.

The model plume was observed to be attached to the surface surrounding the jet exit and become entrained behind the stack when the wind speed approached the jet exit velocity. Even with entrainment behind the stack, the buoyancy was observed to give downwind plume rise (Figure 3, U/W_s = 0.83), which satisfies the 2/3 power law but falls below the suggested correlation of Briggs (1975). The width (Figure 5) does not appear to be influenced by entrainment.

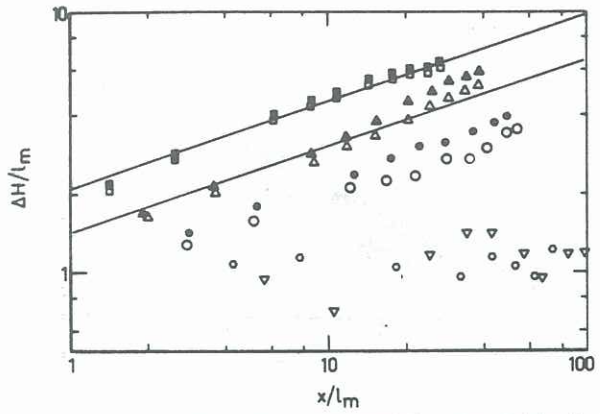

Figure 6 Centreline for jet : model. See Table 2 for symbols. Solid lines (4) with C_2 = 1.44 and 2.1.

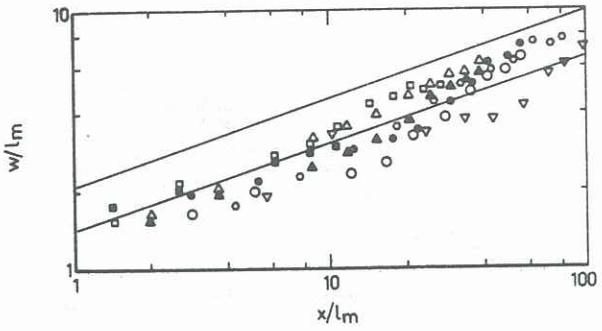

Figure 7 Vertical spreading for jet : model. See Table 2 for symbols. Solid lines (4) with C_2 = 1.44 and 2.1.

The model plume rise, for a non-buoyant jet, using a non-dimensionalised momentum length scale, Figure 6, satisfies the 1/3 power law of (4). The agreement between C_2 and the range 1.44 < C_2 < 2.1 suggested by Fisher et al (1979), their table 9.8, is poor for U/W_s = 0.42. When U/W_s is about 0.6 or larger, the jet was observed to attach to the surface surrounding the jet exit and become entrained behind the stack. There does not appear to be any increase in ΔH due to momentum effects further downstream after the jet is entrained behind the stack. The spread of the non-buoyant jet for all flows appears to satisfy the 1/3 power law of (4), Figure 7, and the data clusters about C_2 = 1.44.

CONCLUSIONS

Analysis of plume rise data from a power station stack and a 1/440 scale model indicates several important features. Non-dimensionalising the plume rise using an appropriate buoyancy length improves the agreement between model and prototype. Both buoyant plume rise satisfies the 2/3 power law. The plume rise is approximately equal to the vertical spread for both model and prototype. Breakup of the power station plume is calculated to occur between 1 and 4 km from the stacks, but at a slightly longer distance than was determined from observational tracking (1.5-2.5 km). The model indicates that when U/W_s is larger than 0.7 the plume is entrained behind the stack and that buoyancy still induces plume rise which satisfies the 2/3 power law. Plume rise from the non-buoyant jet from the model satisfies the 1/3 power law.

ACKNOWLEDGEMENTS

AJC acknowledges the study leave support from the Universities of Newcastle and Canterbury, Australian Research Grants Scheme support and funding from the N.S.W. State Pollution Control Commission.

REFERENCES

BRIDGMAN, H. A. and CHAMBERS, A. J. (1981) Air Quality in the Middle Hunter Valley : The Intensive Study Periods, Report TN FM 60, Department of Mechanical Engineering, University of Newcastle.

BRIGGS, G. A. (-975) Plume Rise Prediction, in Lectures on Air Pollution and Environmental Impact Analysis : Workshop Proceedings. Boston, Mass., American Meteorological Society, 59-111.

CHAMBERS, A. J. and BRIDGMAN, H. A. (1983) Air Quality in the Middle Hunter : The Extensive Study Periods, Report TN FM 83/1, Department of Mechanical Engineering, University of Newcastle.

DEARDORFF, J. W. and WILLIS, G. E. (1975) A Parameterization of Diffusion into the Mixed Layer, J. Appl. Meteorol., 14, 1451-1458.

FISHER, H. B., LIST, E. J., KOH, R. C. Y., IMBERGER, J. and BROOKS, N. H. (1979) Mixing in Inland and Coastal Waters. New York, Academic Press.

FLAY, R. G. J. (1978) Structure of a Rural Atmospheric Boundary Layer Near the Ground. Ph.D. Thesis, Department of Mechanical Engineering, University of Canterbury, New Zealand.

HANNA, S. R., BRIGGS, G. A. and HOSKER, R. P. (1982) Handbook on Atmospheric Diffusion. Report DOE/TIC-11223, Technical Information Center, U.S. Department of Energy.

JACKSON, P. S. (1980) The Dynamic Behaviour of Propeller Anemometers. Proc. 7th Australasian Conference on Hydraulics and Fluid Mechanics, 139-142.

RAINE, J. K. (1974) Modeling the Natural Wind : Wind Protection by Fences. Ph.D. Thesis, Department of Mechanical Engineering, University of Canterbury, New Zealand.

VENKATRAM, A. (1978) Estimating the Convective Velocity Scale for Diffusion Applications, Boundary-Layer Meteorology, 15, 447-452.